

**FUNDAMENTAL ASPECTS OF
ION TRANSPORT IN SOLID ELECTROLYTES**

B. V. Ratnakumar and S. R. Narayanan

Energy Storage Systems Group

Jet Propulsion Laboratory, California institute of Technology

4800, Oak Grove Drive, Pasadena, California 91109

CONTENTS

1.0 Introduction

2.0 Defects and Disorders

2.1 Types Of Defects

2.2 Expressions for Defect Concentration

2.3 Lattice Disorder and Association of Defects

3.0 Structural Features

4.0 Mechanisms of ion transport

4.1 Microscopic Aspects of Diffusion- the Jump Mechanism

4.2 Models of Ionic Motion

4.3 Phenomenological Aspects of Diffusion

4.4 Diffusion Coefficients

4.5 Methods of Measurement of Diffusion Coefficients

5.0 Conduction

5.1 Phenomenological Description of Conduction

5.2 Measurement of Total Ionic and Electronic Conductivity

5.3 AC Methods

5.4 Separation of Ionic and Electronic Conductivity

5.5 Method of Measurement of Transference Numbers

6.0 Thermodynamic Measurements on Solid Electrolyte cells

6.1 Thermodynamic Parameters from Electrochemical cells

6.2 Determination of Thermodynamic Parameters

6.3 Comparison with Other Methods

6.4 Kinetic Measurements

6.5 Limiting Factors

7.0 References

1.0 INTRODUCTION

Solid electrolytes (also termed as superionic solids or fast ion conductors) are characterized by high electrical conductivity, comparable to concentrated liquid electrolytes or even molten salt electrolytes, made possible by rapid transport of ions in the crystalline lattice. The electronic conductivity is small with an electronic transference number (t_e) less than 10^{-4} . A semi-empirical rule formulated by Heyne^[1] stipulates the allowable values for the electronic band-gap in good solid electrolytes to be higher than $t/300$ eV, i.e., a low electronic conductivity of $10^{-6} \Omega^{-1} \text{cm}^{-1}$ at any temperature - a necessary but not sufficient condition. Such superionic solids paved the way for the development of solid state electrochemistry or solid state ionics and also furthered progress in related technologies such as galvanic cells (batteries), fuel cells capacitors, electrochromic devices and sensors.

The conductivity of superionic solids (e.g. RbAgI_5 - $0.27 \Omega^{-1} \text{cm}^{-1}$ @ room temperature) is typically many orders of magnitude higher than of commonly known ionic solids, (e.g. NaCl , KCl - $10^{-16} \Omega^{-1} \text{cm}^{-1}$). Many ionic solids exhibit such high electrical conductivity above a certain temperature, often associated with distinct structural change (e.g. AgI). Further, structures that permit rapid ion transport are generally disordered channeled or layered^[2].

Microscopically, the ionic conductivity in solids is caused by the existence of defects or disorders. A perfect crystal of an ionic compound would be an insulator^[3]. Based on the types of defects or disorders, the superionic solids can be classified as follows:

Point defect (zero dimensional) type : Here, the concentration of the point defects is 10^{20}cm^{-3}

Molten - sub-lattice type: a case of liquid-like molten sub-lattice, in which the number of ions of a particular type is less than the number of sites available for them. The number of mobile ionic charge carriers is 10^{22}cm^{-3} . These are often marked by a channeled or layered structure.

Despite the fact that cations as well as anions can move in the solid lattice, mobility of cations is generally favored due to their small ionic size. Many of the known superionic solids are cationic conductors and especially of small size, e.g. Li^+ , Na^+ , K^+ . Also many of the solid electrolytes involve a monovalent ion, owing to relatively strong coulombic interactions between divalent or trivalent ions with the lattice. This is an oversimplification of the underlying mechanism. A more rigorous correlation between the ionic conduction and the structural aspects of the solid electrolytes has been attempted recently^[4-7].

2.0 DEFECTS AND DISORDERS

2.1 Types of Defects

The lattice defects present in an ionic solid are conventionally represented using Kroger-Vink notation, which specifies the nature, location and effective charge of a defect relative to the neutral unperturbed lattice. The various kinds of point imperfections possible (Fig. 1.1) in an ionic crystal (MX, M and X are monovalent) taking into account the requirement of charge neutrality are as follows.

- (i) **Vacancies:** a missing M^+ ion in a pure binary compound missing from its normal site depicted as V'_M . Likewise a vacant anion site is represented by V''_X (V° stands for vacancy, the subscript for the missing species and the superscript for the charge, prime for effective negative charge and dot for positive charge).
- (ii) **Interstitials:** An ion M^+ or X^- occurs in an interstitial site denoted as M^*_i or X'_i . The term vacancy (or interstitial) defect may be understood to occur if in a volume element of the lattice, a particle is missing (or contains an excess particle) with respect to the ideal lattice, independent of whether at the point or in its immediate vicinity, particles deviate from their normal position or not. In other words any such defect is believed to cause a certain distortion of the lattice in the immediate neighborhood.
- (iii) **Misplaced atoms :** an atom M occupying a normal X site or vice versa, M_X or X_M .
- (iv) **Schottky defects :** a cation vacancy together with an anion vacancy ($V'_M V''_X$) predominantly present in alkali halides. In this vacancy mechanism of conduction, positive and negative ions leave their normal sites to jump into vacancies.
- (v) **Frenkel defect :** a cation vacancy together with an interstitial cation ($V'_M M^*_i$) as in silver halides. Anti-Frenkel defects ($V''_X X'_i$) occur in ThO_2 and CaF_2 . If the migration of atoms takes place by jumps of interstitial from interstice to interstice, it is termed an interstitial mechanism. When an interstitial jumps to a normal site pushing the atom at it to another interstice, it is termed an interstitialcy mechanism.
- (vi) **Impurities :** Aliovalent impurities substituting for a normal or interstitial site. Impurity cations of higher (than host cation) valence generates impurity cation + interstitial anion ($L^\bullet_M X'_i$) or impurity cation + cation vacancy ($L^\bullet_M V'_M$) defects. With a lower valence impurity, it is possible to get an impurity cation + anion vacancy or impurity cation + cation interstitial defect.

A summary of the types of defects established in different ionic crystals is given in Table 1. In general, defect types based on interstitial anions (type ii, iii and vi) are less likely than their cation counterparts, due to a relatively closer packing of anions in most ionic solids.

2.2 Expressions for Defect Concentration

The ionic conductivity as well as the diffusion coefficient are governed by the concentration of defects. The concentrations of the defects of both Schottky and Frenkel type, under various conditions can be expressed in terms of the thermodynamic parameters corresponding to the defect formation as shown below^[8]:

i) Pure crystal

Consider the case of Schottky defects. Let the mole fractions of positive and negative ion vacancies be x_1 and x_2 and their numbers be n_+ and n_- respectively.

$$n_+ = n_- = N \exp(-G_s / K T) \quad (1.1)$$

$$\begin{aligned} x_1 x_2 = x_o^2 &= \exp(-G_s / K T) \\ &= \exp(S_s / K) \exp(-H_s / K T) \end{aligned} \quad (1.2)$$

where G_s , S_s and H_s are the Gibbs energy, entropy and enthalpy respectively, of the formation of a Schottky pair. 'N' is the number of cation or anion sites. For a pure crystal, the charge neutrality condition is written as

$$x_1 = x_2 = x_o$$

The Frenkel defects can likewise be expressed as

$$n_F = (N N')^{1/2} \exp(-G_F / 2 K T) \quad (1.3)$$

where N is the number of interstitial sites and G_F is the Gibbs energy for formation of Frenkel defects.

ii) Doped Crystal

If an ionic crystal is doped by an aliovalent impurity (e.g., Ca^{++} in NaCl), additional cation vacancies are produced to compensate for the charge difference. The charge neutrality equation would then be

$$x_+ = x_2 + c_1 \quad (1.4)$$

where c_1 is the mole fraction of the divalent impurity.

From equations (1.1), (1.2) and (1.4), we get

$$x_1 = 1/2 c_1 \{ 1 + (2 x_0 / c_1)^{1/2} + 1 \} \quad (1.5a)$$

$$x_2 = 1/2 c_1 \{ 1 + (2 x_0 / c_1)^{1/2} - 1 \} \quad (1.5b)$$

For a large dopant concentration, i.e., $c \gg X$, the above equations reduce to $x_1 = c$ and $x_2 = x_0^2 / c$. For small concentrations, on the other hand, the concentrations reduce to the pure crystal values as expected, i.e., $x_1 = X_2 = x_0$.

For a divalent anion impurity with a concentration C_2 , The charge neutrality condition becomes

$$x_1 + c_2 = x_2 \quad (1.6)$$

and the values of x_1 and X_2 would be

$$x_1 = 1/2 c_2 \{ 1 + (2 x_0 / c_2)^{1/2} - 1 \} \quad (1.7a)$$

$$x_2 = 1/2 c_2 \{ 1 + (2 x_0 / c_1)^{1/2} + 1 \} \quad (1.7b)$$

The extra charge on the divalent cation impurity may also induce an association of the oppositely charged cation vacancies. Since these complexes will not contribute to the conductivity, it is essential to know and correct for the number of these associated impurity - vacancy pairs.

2.3 Lattice Disorder and Association of Defects

The lattice disorder could be isotropic as in AgI, doped-ZrO₂ and ThO₂, or in one direction as the crystals with a tunnel-type structure^[9] (e.g. tungsten bronze) or in two directions as in crystals with a plane containing a loose, random packing of atoms sandwiched between close-packed planes (e.g. β -alumina type^[10]). The defects resulting from aliovalent impurities are in general randomly distributed over the appropriate sub-lattice sites and often carry a net charge. Electrostatic attraction between such charged defects may promote the formation of defect pairs or large clusters that may be electrically neutral or carry a net charge. Due to such association of defects, the concentration of free or quasi-free defects doesn't increase linearly with increasing defect concentration and may decrease with decreasing temperature. It follows from Lidiard's analysis^[3] that at a given temperature, the conductivity varies with the impurity addition at first linearly (up to about 1% defect concentration) and then at a decreasing rate until it becomes nearly asymptotic. Beyond about 3% - 4% of defect concentration, however, the above analysis appears to breakdown, since the conductivity decreases with increasing defect concentration. At these high defect contents, clustering or ordering of defects starts. Recent calculations based on near-neighbor interactions^[11] show that the effective charge carrier concentration

goes through a maximum at a certain dopant level in massively defective solids. When very large defect contents are involved, new compounds can occur.

3.0 STRUCTURAL FEATURES

The potential utility of the solid electrolyte materials for a wide range of technological applications was brought out by Wagner and coworkers [12-14]. Further impetus to this field was provided by two family of materials exhibiting unusually high ionic conductivities at surprisingly low temperatures. These were :

a) Silver-conducting ternary silver iodides : Bradley and Greene^[15,16] and Owens and Argue^[17] had described solid electrolyte of the form MAg_4I_5 with conductance at ambient temperature in excess of 10 S m^{-1} , the same value of conductance of a molar KCl aqueous solution.

b) Alkali metal-conducting β -aluminas : Yao and Kummer^[18,19] showed that a single crystal of β -alumina exhibited rapid diffusion (diffusion coefficient of sodium ions of $1 \times 10^{-9} \text{ m}^2/\text{s}$ at 300°C - a value comparable to that in molten NaNO_3) of univalent cations in a plane perpendicular to the c-axis.

The β -alumina type materials were of particular importance due to a wide variety of fast ionic solid materials that emerged therefrom and to the formulation of a new battery system, sodium-sulfur^[20] of high specific power and power with the solid electrolyte acting as a separator between liquid reactants. Other battery systems in this family emerged recently (sodium metal chloride batteries) constitute solid transition metal chloride in chloroaluminate melts as cathodes [21-23].

In general, solid electrolytes with Schottky disorder, in which ionic transport occurs by the motion of vacancies such as alkali halides have high activation enthalpies and low ionic conductivities. On the other hand, the materials with Frenkel disorder, such as some silver and copper halides, in which ionic transport occurs by the motion of interstitial species have low activation enthalpies and high ionic conductivities. The third group of materials called fast ionic or supersonic conductors exhibit very high ionic conductivities and unusually low values of activation enthalpy. Many of the solid electrolytes may fall in between these three categories or even shift from one type of behavior to another.

A number of structural features have been found to characterize the solids which have rapid ionic transport and to distinguish them from the more usual ionic crystals. Typically, their structures are not close-packed but contain networks of ion-sized passageways consisting of interconnected polyhedra of the fixed ions, through selected mobile ions may move. In general, the number of sites available for the mobile ions is much larger than the number of mobile ions themselves; hence the solid has a highly disordered structure. The high conductivity is brought about by a combination of mobile particles and a low enthalpy of activation for ion motion from site to site.

It is now clear that the materials that exhibit fast ionic conduction have special characteristics related to their crystal structures. Several reviews have appeared^[24-37] dealing with such fast ionic conductors. These materials are broadly classified below based on their characteristic features related to the crystal structure.

Interstitial motion in body centered cubic (BCC) structure

One of the first materials in this class^[38] was AgI above 146°C containing BCC arrangement of I⁻ ions with which Ag ion moves interstitially^[39]. The high temperature phase of Ag₂S has also similar structure that permits Ag ions to move interstitially through the tunnels in the body-centered cubic array of sulfur ions^[12].

Interstitial motion in rutile structure

The rutile (TiO₂) structure has a tetragonal symmetry in which the cations are octahedrally coordinated by anions and these octahedra are joined into a three dimensional framework by sharing corners such that each anion is adjacent to these cations. This arrangement produces a relatively open tunnel in the 'c' direction made up of a string of distorted edge-sharing tetrahedral sites that are empty in the ideal structure. Motion of ions residing in these sites would involve passing through a two-coordinate aperture (the shared edge) similar to that in the α -AgI structure. In such structures, lithium ion^[40,41], H⁺ and D⁺ ions^[42,43] are quite mobile and the ionic transport is highly directional.

Other materials with unidirectional tunnels

Several other materials containing unidirectional crystallographic tunnels within which ionic species can be quite mobile, exist either primarily as ionic or as mixed conductors. Some examples are alkali metal vanadium oxide bronzes^[44], the quaternary titanium oxide hollandites^[45-47], the alkali aluminosilicate β -eucryptite^[48-51] and the lithium titanium oxide phase ramsdellite.

Materials with fluorite and antiferite structures

The most common of the fast ion conductors with fluorite (CaF₂) structure is the ZrO₂ family in which the mobile species are the oxide ions. Doped ZrO₂ has been used in a number of applications such as oxygen sensors^[27, 52-54]. Another material of special interest because of its large anionic (fluoride ion) conductivity is PbF₂^[55-67]. Among the materials having the antiferite structures, Li₅AlO₄, Li₅GaO₄, Li₆ZnO₄ exhibit high lithium ion conductivity at moderate temperatures^[68]. It is thus possible to find high values of both anionic (in the fluorite structure) and cationic (in the antiferite) transport in these unique crystal structures.

Materials with layered structures

The β -alumina family is the most important of the group of materials with layer-type crystal structures. Comprehensive reviews of these materials are presented by Kummer^[10], Kennedy^[69] and Collongues et al^[70]. The crystal structure of hexagonal β -alumina consists of four cubic close-packed layers of oxygen with 3 Al^{3+} ions occupying some of the resulting octahedral and tetrahedral positions between each pair of oxygen layers - an arrangement similar to the spinel, MgAl_2O_4 . These spinel blocks are separated by basal planes containing a loose packing of Na and O ions, the spaces between the mirror planes being 1.12 nm. Another structure that has been found to exhibit rapid anionic transport is the tysonite (LaF_3), which is used in fluoride ion selective electrodes^[71]. Materials with this structure based on CCF_3 were found to have higher fluoride ion conductivity^[72]. Lithium nitride also has a layered type structure but with a cationic conductivity. The conductivity for lithium ions is fairly and anisotropic^[51, 73]. There exist two types of sites for Li ions, one in the hexagonal Li_2N layers and the other in the relatively open intermediate layers, where they form N-Li-N bridges^[74]. Finally there exist several mixed conducting materials that are layered in structure similar to CdI_2 , e.g., transition metal chalcogenides. Here, the cation is bonded to the lattice by van der Waals forces, rather than by ionic bonding as in β -alumina. These materials are used as cathode materials in rechargeable lithium cells.

Materials with three dimensional arrays of tunnels

One of the pioneering class of compounds in this category of solid electrolytes containing atomic-sized tunnels oriented in three directions and providing isotropic ionic transport is ternary silver iodides of the RbAg_4I_5 family^[15, 16] 1751. Several such groups of materials having skeleton or network structures composed of arrays of corner and edge-shared tetrahedra and octahedra are being developed at various laboratories.

Structures with isolated tetrahedral

Examples in the category of compounds with characteristic isolated tetrahedral anionic groups between which cations move include Li_4SiO_4 ^[76], Li_4GeO_4 ^[77, 78] and several alkali metal chloroaluminates having structures with alkali metals in between isolated AlCl_4 groups.

It is clear from the above discussion that the fast ionic conduction in solids is rather sensitive to the crystallographic features. Though the presence of unusually large concentration of mobile species was originally viewed as the dominant factor, the static part of the crystal structure plays a significant role in determining the nature and ease of ionic transport.

4.0 MECHANISMS OF ION TRANSPORT

In solid electrolytes, ions are in perpetual random movement in all possible directions (Brownian motion) from a lattice point to a vacancy or interstitial site, or from one interstitial site to another, even in the absence of an electric field. By this random movement the concentration of ions and defects are rendered uniform throughout the solid, and this process is referred to as *diffusion*. When an electric field is impressed on the solid, the ions still randomly move about, but migrate as a whole along the direction of the electric field manifesting as ionic conduction. Thus diffusion and migration of ions via defects constitute the basic processes of ionic conduction in crystalline ionic solids. In amorphous polymeric materials ionic diffusion is possible by local motion of polymer chains. Hence a liquid like character attainable above the glass transition temperature of the polymer becomes necessary for ionic diffusion.

4.1 Microscopic Aspects of Diffusion - the Jump Mechanism

During diffusion and ionic conduction, ions must move through the lattice by some jumping process. A direct cation-anion exchange is ruled out and the ion transport is mediated through defects. The ion transport is thus governed by the jump probability of an ion into a defect. This in turn is proportioned to (Beniere 1972)^[78]

- a) the probability for the ion to jump into the defect in a given direction in unit time, which is the jump frequency.
- b) the probability that a given site has a defect on a nearest neighbor site, i.e., the product of the number of nearest neighbor sites and the mole fraction of the defects.

The jump frequency ' ω ' depends upon the potential barrier experienced by the ion (Fig. 1.2). Assuming that the Einstein model to be applicable, i.e., that the ions are vibrating harmonically around their equilibrium positions with a vibrational frequency, ν_0 , the expression for the jump frequency of a point defect is of the form^[79]

$$\omega = \nu_0 \exp(-\Delta G / K T) \quad (1.8)$$

where ΔG is the free energy of migration, ' ω ' can be expressed in terms of ΔH (enthalpy of migration) and ΔS (entropy of migration) as

$$\omega = V \cdot (\Delta S / k) \exp(-\Delta H / K T) \quad (1.9)$$

This is an expression for the thermodynamic equilibrium allowing an equal number of jumps in both left and right directions. However, such is not the case if a gradient is generated due to differences in either applied electrochemical potential or concentration (chemical potential). In the case of an imposed electric field, the potential energy experienced by the interstitial ion jumping one interstitial position to another is asymmetric

as shown in Fig. 1.3. Due to the electric field, E , an additional term, $-q E x$ is added to the potential energy term, where q is the charge on the interstitial ion and x is half the interionic distance, a . The subsequent saddle point energy decreases by an amount $1/2qaE$. A jump in the direction of the field would therefore take place with increased probability:

$$\omega' = v_0 \exp [-(\Delta G - 1/2 q a E) / K T] \quad (1.10)$$

and a jump against the field occurs with reduced probability,

$$(1)'' = v_0 \exp [-(\Delta G + 1/2 q a E) / K T] \quad (1.11)$$

The net number of ions moving per unit volume in the direction of the field,

$$n' = n (\omega' - \omega'')$$

$$n \omega q a E / k T$$

assuming $q a E \ll k T$. Here, n is the number of interstitial ions per unit volume. The current density, j , (which is the amount of charge passing per unit area per unit time) is given by

$$j = n a^2 q^2 \omega E / k T \quad (1.12)$$

The expression for the ionic conductivity, σ , is expressed in terms of the jump frequency as

$$\sigma = j / E$$

$$= n a^2 q^2 \omega / k T = n q \mu \quad (1.13)$$

where μ is the mobility, given by

$$\mu = a^2 q \omega / k T \quad (1.14)$$

Finally, an additional numerical factor is added to the above equation to account for the fact that the charge carrier can jump to multiple forward positions (e.g., 4 for NaCl) in the lattice. Similar expression holds good for the vacancy or interstitially mechanism. The net ion transport induced by a concentration gradient is termed as diffusion and is dealt in detail in Section 4.3.

4.2 Models of Ionic Motion

Development of models of ionic motion may be considered to have place in three stages. Of the early transport mechanisms suggested, apart from the free ion model of Rice and Roth^[80], most tried to extend the *above simple hopping* model from its successful application to the defect conductivity mechanism to systems where the mobile ion concentration was high. In the second group of theories, recognition was given to *co-operative motion*, where the influence of mobile ions on one another was taken into consideration. Finally, for systems in which the flight time between sites was shown by spectroscopic methods to be of the same order as the dwell time, motion was characterized in terms of quasi-liquid sub-lattice behavior. Only one microscopic model has been developed specifically for describing the transport mechanism in polymer electrolytes, namely the dynamic bond percolation model^[81-83]. This theory is based on the principle that local segmental mobility of the polymer host controls the ionic conductivity and diffusion processes. Occasional independent hopping of ions is assumed to occur in addition, however, only rarely. In a fixed configuration of the polymer host with ions all in low energy equilibrium positions, the probability of an ion hopping at a characteristic rate can be visualized as a percolation process governed by the availability of accessible empty ion sites. However, in the case of a polymer host above its glass transition temperature, the chains are constantly in motion altering and readjusting the probability values. Thus availability of empty sites get renewed in a time scale determined by the polymer motion. For observations greater than this time scale, a diffusive behavior would be observed. For shorter time scales the motion would be equivalent to hopping. Static percolation would be observed if the polymer motion is extremely slow. When polymer motion rates increase the diffusion coefficients and conductivity increase monotonically until the ion-transport changes to ion-hopping type independent of the chain motion. Such a condition is called renewal saturation. The full implementation of this model awaits understanding of ion-ion interactions in ion hopping, experimental input on relaxation processes (such as NMR data), and extension of the lattice formalism to describe amorphous systems.

4.3 Phenomenological Description of Diffusion

Despite the fact that the processes of diffusion and migration are microscopic phenomena governed by fundamental interactions between ions and lattice and defect sites, a phenomenological description based on concentration of diffusing species, electric field gradient, and experimentally accessible quantities such as diffusion coefficients and ionic mobility is of immense practical value.

Fick's laws and diffusion equations

When a concentration gradient exists in a solid, diffusion results in a net ionic flux in the direction which tends to make the concentrations uniform. In 1855, Fick stated that the diffusion flux J (defined as material flow per unit time) is proportional to the

concentration gradient. Thus, for a concentration gradient in one dimension we have Fick's first law as,

$$J_x = -D \left(\frac{\partial C}{\partial x} \right) \quad (1.15)$$

where D is called the diffusion coefficient. The negative sign in Eq. 1.15 is because a negative concentration gradient results in a positive diffusion flux.

When the concentration gradient varies with x, there is difference in the fluxes at x and x+Ax, given by $(J_x - J_{x+\Delta x})$. In a time Δt , there occurs an accumulation of material given by $(J_x - J_{x+\Delta x}) \cdot \Delta t$. This material accumulation manifests itself as a change in concentration with time, $\Delta C (= C_{t+\Delta t} - C_t)$, or total material accumulation of $\Delta C \cdot \Delta x$. Thus

$$(J_x - J_{x+\Delta x}) \cdot \Delta t = \Delta C \cdot \Delta x$$

or in the differential form,

$$\frac{\partial C}{\partial t} = -\frac{\partial J_x}{\partial x} \quad (1.16)$$

Combining this with the first law (Eq. 1.15) we have,

$$\frac{\partial C}{\partial t} = \frac{\partial \{D \left(\frac{\partial C}{\partial x} \right)\}}{\partial x} \quad (1.17)$$

If D is a constant, Eq. (1.17) maybe written as ,

$$\frac{\partial C}{\partial t} = D \cdot \frac{\partial^2 C}{\partial x^2} \quad (1.18)$$

and may be generalized into the three-dimensional isotropic diffusion equation.

$$\frac{\partial C}{\partial t} = D \left(\frac{\partial^2 C}{\partial x^2} + \frac{\partial^2 C}{\partial y^2} + \frac{\partial^2 C}{\partial z^2} \right) \quad (1.19)$$

Solutions for Eq. (1.18) yield concentration distribution with time for a given set of boundary and initial conditions. For example let us consider diffusion either direction ($-\infty < x < \infty$) from a plane source containing at $t=0$ an amount M of a substance. The concentration distribution changes with time and is given by:

$$C(x, t) = \left\{ \frac{M}{2(\pi Dt)^{\frac{1}{2}}} \exp \left\{ -\frac{x^2}{4Dt} \right\} \right\} \quad (1.20)$$

Thus diffusion under these conditions proceeds symmetrically from the origin ($x=0$) and the simple average position of the diffused substance is always the origin. However, the mean square X^2 of the distance at any time t can be derived to be equal to $2Dt$. Thus the mean square increases proportionally with time and the constant of proportion is $2D$. Therefore, D is a measure of the spreading velocity of the substance. Another typical example of a diffusion in ionic solids is characterized by the following conditions:

Semi-infinite (i.e. $0 > x > \infty$) and linear (one-dimension) diffusion from a surface maintained always at a constant concentration C_0 . At $t=0$ and $x > 0$, $C=0$. Under these conditions the concentration distribution is given by :

$$C = C_0 (1 - \operatorname{erf}\{x/2\sqrt{Dt}\}) \quad (1.21)$$

for all $t > 0$ where erf denotes the error function.

Analytical solutions for various sets of boundary and initial conditions are given by Crank^[84], and the mathematically equivalent problems in heat transfer by Carslaw and Jaeger^[85]. The diffusion process in which the concentration changes with time is called non-stationary diffusion, while that which is not time dependent is called stationary diffusion. For stationary diffusion, thus $\partial C/\partial t = 0$ and thus from Eq. 2.2 $\partial J/\partial x = 0$ and therefore, J is a constant.

Modified Fick's first law and the Nernst-Einstein equation

In a more generalized interpretation of diffusion, Einstein^[86] and Hartley^[87] believed that the true driving force for diffusion was the chemical potential gradient, instead of the concentration gradient claimed in Fick's first law. Such an interpretation accommodates the thermodynamic non-ideal character of real systems. Chemical potential μ of a system is defined as the partial molal Gibbs free energy and has the units J mole⁻¹. This generalized description of diffusion is embodied in Wagner's theory^[88] for ion transport in crystals. The flux J_i of a particular species i is then given by

$$J_i = -C_i B_i (1/N) \partial \mu_i / \partial x. \quad (1.22)$$

where C_i is the concentration (mole cm⁻³), B_i is the absolute mobility (cm² J⁻¹ S⁻¹) and N is the Avogadro's number. The absolute mobility (or mechanical mobility as it is sometimes called) is thus the migration velocity of the species per unit energy gradient. The chemical potential is related with activity a_i of species i and the activity coefficient γ_i as

$$\begin{aligned} \mu_i &= \mu^\circ + RT \ln a_i \\ &= \mu^\circ + RT \ln \gamma_i + RT \ln C_i \end{aligned}$$

The gradient of the chemical potential is then given by

$$\partial\mu_i/\partial x = RT \{ 1 + (\partial \ln \gamma_i / \partial \ln C_i) \} (1/C_i) \cdot \partial C_i / \partial x \quad (1.23)$$

Substituting the above relation for $\partial\mu_i/\partial x$ in Eq. (1.22) and comparing with Fick's first law (Eq. 1.15), we find

$$D_i = B_i kT \{ 1 - (\partial \ln \gamma_i / \partial \ln C_i) \} \quad (1.24)$$

This relation between diffusion coefficient, absolute mobility and the concentration of the diffusing species describes ideal and non-ideal systems and is called the *Nernst-Einstein equation*. The diffusion coefficient defined by Eq. 1.24 is referred to as the component diffusion coefficient. When $\gamma_i=1$ as in an ideal solution,

$$D_i = B_i kT \quad (1.25)$$

and then D_i is equal to that defined by Fick's first law.

4.4 Diffusion Coefficients

Self and isotope diffusion coefficient

The measure of random (**Brownian**) motion of ions or atoms is usually called the self-diffusion coefficient. However, for practical reasons sometimes the diffusion of the isotope of the ion or atom (called tracer) is studied and therefore the diffusion coefficient so obtained is termed the isotope or tracer diffusion coefficient. Thus the self diffusion coefficient is related to the isotope diffusion coefficient by a correlation factor which is usually less than unity.

Defect diffusion coefficient

In the example of vacancy diffusion, if the concentration ratio of vacancies to ions on the lattice site is 1:100, on average an ion jumps once for every hundred jumps of a vacancy. This leads up to a relation between the diffusion coefficient of the vacancy, D_v and the self-diffusion coefficient, D as

$$D_v C_v = D C$$

C_v is the concentration of the vacancies and C the concentration of the lattice sites.

Chemical diffusion coefficient

When ions are involved in chemical reactions such as insertion into a lattice to form a new phase or in exchange processes where one type of ion replaces another, changes in stoichiometry, the diffusion of these ions is accompanied by a solid state chemical change whose rate is controlled by the diffusion. Such diffusion processes could involve the participation of more than one chemical or ionic species and is termed chemical diffusion.

The chemical diffusion coefficient can be thus be related to the self diffusion coefficient by a factor proportional to the interactions in chemical diffusion (Wagner¹⁹⁵¹).

Haven ratio

Over a wide range of temperatures, experimentally measured diffusion coefficients often obey the relation

$$D = D_0 \exp (- \Delta E / k T)$$

where D_0 is a constant, pre-exponential factor and ΔE is the activation energy for diffusion. The diffusion coefficient D and the electrical conductivity are related, as will be shown later in section 5.1, by the Nernst-Einstein relation :

$$\sigma / D = N q^2 / k T \quad (1.26)$$

where q is the charge of the moving species and N is their number per unit volume. The diffusion coefficient, $D_{(calc)}$ calculated from the measured value of the conductivity as

$$D_{(calc)} = (k T / N q^2) \sigma \quad (1.27)$$

is generally different from the value directly measured value, D , e.g., by tracer diffusion coefficient. The disagreement between the two is attributed to the fact that in the electrical conductivity measurements under applied field, the successive jump directions of defects are uncorrelated with one another, while such is not the case in the absence of electric field. The correlation between both the diffusion coefficients is given by the relation :

$$H_r = D / D_{(calc)} \quad (1.28)$$

and is called the 'Haven Ratio'. This is almost the same as the theoretical correlation factor 'f' introduced in the equation relating the diffusion coefficient with the jump frequency and jump length.

4.5 Measurement of Diffusion Coefficients:

A wide variety of methods have been used for solving Fick's equations^[90-92]. There are two main approaches to theory : a) the atomistic approach where the atomic nature of the diffusing species is specially considered and b) the continuum approach where the atomic nature is ignored. The former relates the diffusion coefficient to quantities like atom jump frequency, relaxation time etc. and the later relates to the initial and final state (concentration) of the system. The experimental methods used for the measurement of diffusion coefficient are related to the above methods of treating the diffusion phenomenon and can be grouped as

Direct method : The mass flow or concentration is measured as a function of either distance or time

Indirect method : The jump frequency or relaxation time is measured to evaluate the diffusion coefficient

$$D = \frac{1}{6} f \lambda^2 \omega \quad (1.29)$$

where λ is the jump length, ω is the jump frequency and f is the correlation factor. The value of the jump frequency can be determined by relaxation measurements like light scattering, NMR, diffuse neutron and x-ray scattering.

The direct methods evaluate the diffusion coefficient by measuring the concentration of the diffusing species as a function of depth of penetration. Such methods are often more reliable and include a wide variety of physico-chemical methods like mass spectrometry, radio-active tracer technique, spectrophotometry etc. The electrochemical methods also fall into this category and are based on measuring the concentration profile through a variation of either electrode potential (chronopotentiometry), reaction current (chronoamperometry) or coulombic charge (chronocoulometry). Among the various direct methods, tracer diffusion technique is generally adopted wherever possible, as irreproducibility may exist in other direct methods.

Tracer method

This method is applicable to a polycrystalline or single-crystal slab of the specimen. The tracer diffusion coefficient of an ion M^+ in a matrix MX is measured by applying a very small amount of a radio-isotope of M on a plane perpendicular to the direction in which the diffusion coefficient is to be measured. The sample is now annealed for a desired time. The distribution of isotopes can be followed by sectioning the samples and estimating the amount of the isotope in each section by radio-counting or by secondary ion mass-spectrometry. Analytical expressions for spatial concentration distribution with semi-infinite boundary conditions can be used to evaluate the diffusion coefficient.

NMR Method

A nucleus with a non-zero nuclear spin quantum number I , when placed in a uniform magnetic field H_0 suffers an energy level splitting into $2I + 1$ discrete levels with equal energy differences of $\Delta E = \gamma \hbar H_0 / 2\pi$, where γ is the gyromagnetic ratio. The gyromagnetic ratio characterizes the nucleus and its environment. The energy absorbed by the nucleus is in the radio frequency range and the phenomenon is called nuclear magnetic resonance (NMR). For an isolated nucleus a sharp line is observed. However, splitting or broadening of lines occurs due to the interaction of the nucleus with its surroundings. So information of the local structure of molecules or atomic groups are hidden in this broad band. As temperature is raised, the thermal motion of atoms results in an average

magnetic dipole interaction causing narrowing of the resonance band, and this phenomenon is called motional narrowing. Motional narrowing of resonance lines can be used to determine the nature of the diffusing species. To determine the diffusion coefficient, the relaxation of the excited state as it recovers by releasing its energy to its surroundings (spin-lattice relaxation), must be observed. The spin-lattice relaxation time when plotted as a function of $1/T$ passes through a minimum value τ_c for a constant applied frequency and at the minimum a correlation time τ_c . Then τ_c can be used to estimate a value of diffusion coefficient which agrees well with the self-diffusion coefficient. Further details on the NMR method are provided by Bannett^[93].

Electrochemical methods

Diffusion coefficients can be determined from galvanic cells employing the solid electrolyte by combining current generation and potential measurements. In this method a perturbation of the concentration gradients of the mobile ionic or electronic species is accomplished by a controlled transient electrical current or potential signal. The attainment of a steady-state concentration gradient following such a perturbation is followed. These methods are described in the following:

Chronoamperometry

In this method, the uniform distribution of the mobile species is suddenly altered at the electrode/electrolyte interface by a potential step. A time-dependent current flow immediately results in response to the concentration gradient until a new and homogeneous composition is reached. The time dependence of the concentration profiles is determined by the diffusion coefficient and the direction of diffusion and geometry of the boundaries. Commonly, experiments are arranged to approximate to linear diffusion to a plane or cylinder. For linear diffusion to a plane of unit area for time $t \ll L^2/D$, where L is the thickness over which diffusion occurs, and for a potential step ΔE , the current density I is given by

$$I = z q N_A \Delta E t^{-1/2} \sqrt{D} / (V_M \pi^{1/2} dE/dy) \quad (1.30)$$

where, z is the charge on the mobile species, q is the elementary charge, V_M is the molar volume, and y is the stoichiometric number. Thus the slope of the plot of I vs $t^{-1/2}$ at short times will be a straight line from which the diffusion coefficient D may be evaluated.

Galvanostatic(or current step) Method

In this method the current is stepped from zero to a constant value I_0 . The concentration changes and diffusion of mobile species results in a time-dependent potential which is measured as a function of time. For short times, the linear diffusion to a plane under a current step I_0 results in a time dependent potential, E expressed as:

$$E = \{ 2 V_M I_0 t^{1/2} dE/dy \} / z q N_A \pi^{1/2} \sqrt{D} \quad (1.31)$$

Thus the slope of E vs. $t^{1/2}$ can be used to evaluate D . Experimentally, an important advantage of this method is that any fixed impedance does not change the shape of the voltage time curve. Thus compensation of the internal resistance drop and exact knowledge of the position of the reference electrode are not crucial to this method. Since the current is the controlled variable the extent of concentration change caused by the method can be calculated for the chosen current. With the potential step method large currents can flow momentarily causing uncontrolled concentration changes. On the other hand the galvanostatic method does not allow determination of the diffusion coefficient from long-time experiments. Variations of the galvanostatic method employing short pulses is reviewed by Weppner and Huggins^[94].

5.0 CONDUCTION

5.1 Phenomenological Description of Ionic Conduction:

Charged particles can migrate even without a concentration if there is an electric field. The flux is called conduction. When an electric field $\partial\phi / \partial x$ is applied on a charge of magnitude Ze the energy gradient $Ze(\partial\phi / \partial x)$ is generated and the flow equation is then given by

$$j = -CBZe(\partial\phi / \partial x) \quad (1.32)$$

The current $I (=ZFj, \text{coulombs cm}^{-2} \text{s}^{-1}, \text{ where } F \text{ is the Faraday constant})$ is given by

$$I = CBZ^2Fe(\partial\phi / \partial x) \quad (1.33)$$

Then we may express CBZ^2Fe as σ and term σ as the conductivity. Combining the above relationship with that of Eq. 1.25 we have

$$\begin{aligned} B &= D/kT \\ &= \sigma / CZ^2Fe \end{aligned} \quad (1.34)$$

thus allowing a calculation of D from σ or vice-versa when one of the values is known.

5.2 Electrochemical Potential Gradient and a Generalized Formalism for Diffusion and Conduction

In the general situation where charges move by diffusion and conduction, the fluxes can be combined and expressed as

$$J = -(cB/N) \partial(\mu + ZF\phi)/\partial x \quad (1.35)$$

where F/N is e .

As a consequence, it would be possible to define a combined driving force due to chemical and electrical gradients $\partial\eta/\partial x$ where η is called the electrochemical potential and is equal to $(\mu + Z F \phi)$ and a generalized flow equation may be expressed as

$$J = -B Z e (\partial\eta/\partial x) \quad (1.36)$$

The generalized description of flux (Eq. 1.36) based on the electrochemical potential can be written for cations, anions and electrons in a crystal as follows:

$$J_+ = -CBZ_1 e (\partial\eta_+/\partial x) \quad (1.37)$$

$$J_- = -CBZ_2 e (\partial\eta_-/\partial x) \quad (1.38)$$

$$J_e = -CB e (\partial\eta_e/\partial x) \quad (1.39)$$

5.3 Measurement Total Ionic and Electronic Conductivity

Direct current measurements

When direct current is passed through an electrolyte or mixed conductor, electrochemical reactions occur that cause compositional changes. However if the compositional changes caused by passage of current are exactly reverse of each other at either electrodes (such a system is referred to as a system of reversible electrodes), then there is no net change in the chemical potential of the system. Irreversible effects of compositional change are also referred to as electrochemical polarization. Thus reversibility is achieved when the electron transfer reactions at the two electrodes are the exact reverse of each other and only one ionic species conducts exclusively. Under these circumstances the flux of anions, cations and electrons is given by:

$$\begin{aligned} J &= J_+ + J_- + J_e \\ &= (\sigma_+ + \sigma_- + \sigma_e)/F \cdot \partial\eta_e/\partial x \\ &= (\sigma_+ + \sigma_- + \sigma_e).E \end{aligned} \quad (1.40)$$

E is the electric field gradient. Thus the total conductivity is obtained as J/E . Therefore, measurement of conductivity by direct current methods requires the use of reversible electrodes. Also, in direct current measurements, since the potential distribution near the electrode contacts are non-uniform, the potential difference is measured between two

points away from the each of the current carrying electrodes and thus the method is also called the four probe method.

Experimental details for the measurements of electrical conductivity and transport properties of solid electrolytes has been reviewed by Rapp and Shores^[95] and Kvist^[96] and more recently by Blumenthal and Seitz^[54].

Alternating current measurements

Alternating currents of small amplitude, in principle do not cause change in the composition of the solid electrolyte and thus the ac. method can be used with non-reversible electrodes (blocking electrodes); Usually, the smaller the amplitude of alternating current, the higher the degree of reversibility. For this reason the ac. method is widely used.

Electrical equivalent circuits for the electrode/electrolyte interface

If a sample is a pure ionic conductor (i.e., $\sigma_e=0$), and the electrodes are inert to any conducting species (i.e., a blocking electrode) the electrode/solid electrolyte interface behaves as a capacitor. In such an interracial capacitor electronic charge stored on the metal electrode is compensated by ionic charges in the solid electrolyte. These two layers of charge are referred to as an "electrical double layer" and the capacitance termed as a "double layer" capacitance. Under these circumstances an equivalent electrical circuit for the electrodes and solid electrolyte sample is given in Fig. (1.4a), where R_s and C_d represent the electrolyte resistance ($1/(\sigma_+ + \sigma_-)$) and the double layer capacitance.

In actual cases, however, charge transfer (which is an electrochemical reaction) always occurs at the electrode/electrolyte interface and is represented by R_t as in Fig. (1.4b). The charge transfer resistance R_t is the linear equivalent of resistive (or polarizing) characteristic of the interface when it sustains an electrochemical charge transfer. When a steady state current i results in a steady-state potential drop of E across the interface, the $\partial E / \partial i$ is termed the faradaic polarization resistance which is the sum of charge transfer resistance R_t and mass transfer resistance R_m . A linear relation between E and i is usually found when the perturbations are less than 5 mV. Unlike charge transfer, the process of mass transfer is *per se* a time-dependent process and thus exhibits transient properties as determined by the diffusion coefficient and concentration of the diffusing species. Transient mass transfer polarization has thus been understood to arise from an impedance (with the equivalent of ladder-type network of capacitors and resistors) and in a commonly encountered case of semi-infinite boundary conditions, termed Warburg impedance^[97]. Thus a generalized equivalent circuit of Fig. (1.4c) with the electrochemical effects at the interface includes the double layer capacitance, charge-transfer resistance and Warburg impedance.

When the distance of separation between the electrodes is small, the geometric capacitance between the electrodes becomes significant and the equivalent circuit should include a geometric capacitance C_g as shown in Fig. (1.4d). Thus the alternating current method can be used not only to obtain the conductivity of solid electrolytes but also investigate the properties of the electrode/electrolyte interface.

Analysis of impedance data

In the alternating current method, a sinusoidal varying potential $E_m \sin \omega t$ (ω equals $2\pi f$ where f is the sinusoidal frequency in Hz) of small amplitude (usually, 5 mV) is applied to the cell consisting of the electrolyte sandwiched between two electrodes. The sinusoidal current that results is shifted in phase by ϕ and is given by $I_m \sin(\omega t + \phi)$. The two terminal impedance, Z (is given by E_m/I_m), and phase angle difference (between the applied sinusoidal voltage and observed sinusoidal cell current), ϕ , are measured as a function of frequency of the applied sinusoidal voltage, ω . In order to represent the variation of Z as well as ϕ together, a plot of $Z \cos \phi$ (also called Z' or Z_{real} or in phase component) vs. $Z \sin \phi$ (also called Z'' or $Z_{\text{imaginary}}$ or out-of-phase component) at various frequencies is commonly presented as impedance data and is referred to as the Cole-Cole or Nyquist plot. Thus in a plot of Z' vs Z'' by definition,

$$Z = \sqrt{(Z')^2 + (Z'')^2} \quad (1.41)$$

and

$$\phi = \tan^{-1}(Z''/Z') \quad (1.42)$$

Because of the nature of the algebra used in such analysis is similar to that employed in the study of complex numbers, such a representation is also called complex plane impedance analysis.

For the electrical equivalent circuit of Fig (1.4a) the impedance Z is given by

$$Z = \sqrt{(R_s)^2 + (1/\omega C_s)^2} \quad (1.43)$$

Thus in a Nyquist plot for Fig (1.4a), Z' is equal to R_s and Z'' is equal to $1/\omega C_s$ at any frequency and thus the value of R_s and C_s can be evaluated.

For the circuit in Fig. (1.4 b), a parallel combination of the charge transfer resistance R_t and double layer capacitance C_d in series with the ionic resistance R_s , Z can be derived from ac theory as

$$Z = \sqrt{\{R_s + R_t/(1 + \omega^2 R_t^2 C_d^2)\}^2 + \{\omega C_d R_t^2/(1 + \omega^2 R_t^2 C_d^2)\}^2} \quad (1.44)$$

Under these conditions, the Nyquist plot takes the shape of a semicircle and the ionic resistance R_s is determined from the value of Z' extrapolated to $\omega = \infty$. At $\omega \rightarrow 0$, $Z' = R_s + R_t$. When $\tan^{-1}(Z''/Z')$ is maximum, the value of $\omega = 1/R_t C_d$. Thus the value of the circuit elements can be calculated.

Recently, the experimental measurement of impedance components in the range 100 kHz - 1 mHz with frequency response analyzers such as the Solartron series 1550, offers very

high sensitivity and remarkable noise rejection capabilities combined with speed and automation.

With measurements from solid electrolyte-electrode systems, it is usual to compare the results with that of a theoretical model to determine the equivalent circuit and the significance of its different components. Macdonald^[98] has developed theoretical models to describe the impedance of a system in a number of different situations applicable to solid electrolytes. Experimental and analytical details of the alternating current method are discussed by MacDonald^[98], Bauerle^[100] and Armstrong^[99]

Despite the successes with the ac impedance methods, these measurements provide little information concerning the intercrystalline effects. Such bulk phenomenon would normally occur in a highly conducting solid in the range of 10^5 - 10^{12} Hz, well outside the range of normal ac equipment. Hedge et al^[101] have therefore pointed out the advantages of low temperature effects to bring the conductivities below 10^4 S m⁻¹ and the conductance dispersion in a more accessible frequency range.

Cole and Cole^[102] introduced the dielectric relaxation function $1 / (1 + j\omega\Gamma_0)^{1-\alpha}$ and showed that this represents a depressed circular arc in the complex impedance plane. The parameter, α , is a measure of the departure from simple Debye behavior, i.e., a measure of the depression of the center of the circle below the real axis. Non-Debye nature due to inter-ionic forces in a disordered interface region or to the existence of surface roughness. Intracrystalline response is reportedly governed mainly by concentration of mobile ions^[101]. Thus materials having relatively ordered structures and small concentration of mobile defects such as β -PbF₂ and AgCl approximate to the ideal ac impedance behavior with perfect semi-circles. On the other hand, the pronounced dispersion with a single crystal β -alumina is attributed to strong interaction among the mobile Na⁺ ions or to a wide distribution of ion jump frequencies reflecting disorder in the conduction plane.

5.4 Separation of Ionic and Electronic Conductivity

In the measurement methods described above both ionic and electronic species are mobile and their total conductivity is measured. For mixed conductors, the electronic conductivity can be separated from the ionic conductivity by the use of a combination of ion-blocking and reversible electrodes. The objective is to block the ionic flow and sustain only electronic conduction. For example a metal electrode such as silver functions as a reversible electrode in contact with silver bromide. A graphite or carbon electrode in contact with silver bromide does not sustain any electrochemical reaction readily with the ions of the electrolyte when polarized positively and thus functions as an ion-blocking electrode. When a direct current is passed through such a mixed conductor as silver bromide and the voltage between the two electrode terminals (carbon as the positive electrode and silver the negative electrode) is less than the decomposition voltage of silver bromide (bromine evolution from bromide does not occur under these conditions), ionic migration cannot be sustained however a steady-state current is observed due to the

electronic conductivity. Choice of polarity that is reverse of that suggested would result in silver deposition at the carbon electrode leading to silver deposition at the carbon electrode converting it into a reversible electrode. In effect, the reversible electrode serves as a potential invariant electrode (electrochemists refer to such an electrode as a reference electrode) and all potential changes at the blocking electrode can be measured with respect to this reference. Since ion transfer is forbidden at the blocking electrode the ionic current in the electrolyte is zero. The steady-state electronic current at various potentials E can be measured and the electronic conductivity for a solid electrolyte of thickness x and area of cross section A calculated from Ohm's Law as :

$$\sigma_e = - \{ x/A \} \partial i_e / \partial E \quad (1.45)$$

This method is known as the Hebb-Wagner technique^[103,104].

5.5 Methods of Determining the Transference Number

For an electrolyte dissociating to give simple cationic and anionic species, the transport number, e.g., of cation t_+ , is defined as the number of faradays of charge carried by the cation across a reference plane (fixed relative to the solvent), when a total of one faraday of charge passes across the plane ^[105]. In conventional electrolyte, experimental techniques such as the moving - boundary methods were sufficiently well developed to allow routine determination of transference numbers with great accuracy. For polymer electrolytes, however, these methods are inapplicable and a number of alternate methods have been developed ^[106-112]. The Tubandt method ^[109] is the technique most commonly applied to conventional solid electrolytes. It is directly based on Faraday's laws and requires weight variations in the electrolyte regions near the two cell electrodes caused by the passage of a known amount of charge, to be measured. It is difficult to apply this method to polymer systems because of the requirement to maintain the electrolyte as a series of non-adherent sections. Leveque et al^[106] were able to carry out such experiment for highly cross-linked networks where the electrolyte could readily be separated into its component sections after the passage of the current. Bouridah et al ^[110] developed a technique based on the measurement of cmf ^[13-14] of a concentration cell formed by contacting two previously thermally activated half cells. This method is experimentally difficult and has the disadvantage of requiring knowledge of the variation of salt activity with the concentration. The most popular technique for transference number measurements in polymer electrolytes is that developed by Sorensen and Jacobsen ^[108] using an analysis of ac impedance of the cell with two electrodes, each non-blocking with respect to the cation. Here, the current flowing through the cell is affected at low frequencies by concentration gradients near the electrodes, which give rise to a characteristic diffusional impedance in the complex impedance plane. The method is, however, often difficult to interpret^[113] and applicable only at high temperatures, since at normal temperatures the frequencies required to show the diffusional part of the impedances are too low to be of practical value. The steady state current method of Blosky et al^[111] is prone to errors due the electrode effects which might significantly affect the potential distributions and the current flowing through the cell. A combination of dc

and ac polarizations has been proposed by Bruce and Vincent^[114] to alleviate the above problem and thus to determine the transference number even when the diffusion coefficients are low and even in the presence of passivating layers on the electrode and slow electrode kinetics.

6.0 THERMODYNAMIC AND KINETIC MEASUREMENTS ON SOLID ELECTROLYTE CELLS

6.1 Thermodynamic Measurements from Electrochemical Cells

A significant amount of data on the thermodynamic properties pertinent to the solid electrolytes, especially oxide systems has been generated from electrochemical cells with solid electrolytes. From the reversible cell potential of such cells, it is possible to obtain values for the Gibbs free energy change ΔG , for the corresponding chemical reaction in the cell^[115].

The use of solid electrolyte-based galvanic cells for determination of the thermodynamic parameters, e.g. free energy of formation of oxides and halides, was pioneered by Kiukkola and Wagner^[13-14] and Peters et al. [116-117]. Wagner [118] derived an expression for the steady state open circuit potential across a compact mixed-conductor oxide.

Consider an electrochemical cell comprising a solid electrolyte MO, wherein oxygen ions (O^{2-}), excess electrons e' and electron holes $h\cdot$ are the charge carriers. Let $\mu'_{O^{2-}}$ and $\mu''_{O^{2-}}$ be the chemical potentials at the electrode/electrolyte interfaces as shown below:



The partial current density, I_i of the species i at any location within the electrolyte may be written as

$$I_i = (-\sigma_i / z_i F) \partial \eta_i / \partial x \quad (1.50)$$

where σ_i is the partial conductivity of species i , z_i is the valence, F is the Faraday constant, x is the distance coordinate and η_i is the electrochemical potential of species ' i '. The electrochemical potential is defined as:

$$\eta_i = \mu_i + z_i F \phi$$

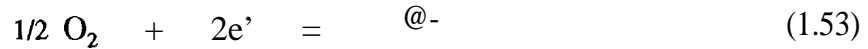
where μ_i is the chemical potential of i and ϕ is the electrostatic potential. The sum of the partial current densities of the oxygen ions, excess electrons and electron holes may be written as

$$I_{O_2} + I_{h\cdot} + I_{e'} = -(\partial\phi / \partial x) (\sigma_{O_2} + \sigma_h + \sigma_{e'}) + \sigma_{O_2} / 2F \\ (d\mu_{O_2} / dx) + \sigma_{e'} / F (d\mu_{e'} / dx) - \sigma_h / F (d\mu_{h\cdot} / dx) \quad (1.51)$$

At open circuit, defined as the limiting case when the sum of partial currents, $I_{O_2} + I_{e'} + I_{h\cdot}$ tends to zero. Thus at open circuit, from the above equation,

$$\partial\phi = (t_{O_2} / 2F) d\mu_{O_2} + t_{e'} / F d\mu_{e'} - t_{h\cdot} / F d\mu_{h\cdot} \quad (1.52)$$

where t_{O_2} , $t_{h\cdot}$ and $t_{e'}$ are the transference numbers of oxygen ions, electron holes and excess electrons respectively, and are given by the ratios of the respective partial conductivities to the total conductivity. In the solid electrolyte MO, the equation may be assumed as



From above equations,

$$d\mu_{O_2} - 2 d\mu_{e'} = \frac{1}{2} d\mu_{O_2}$$

and

$$\partial\mu_h = -\partial\mu_{e'}$$

The above two equations, combined with the conditions that $t_{O_2} + t_{e'} + t_{h\cdot} = 1$ yield

$$\partial\phi = \frac{t_{O_2}}{4F} \partial\mu_{O_2} + \frac{\partial\mu_{e'}}{F}$$

an integration from $x=0$ to L

$$\phi'' - \phi' = \frac{1}{4F} \int_{\mu_{O_2}'}^{\mu_{O_2}''} t_{O_2} d\mu_{O_2} - \partial\mu_{O_2} + \frac{1}{F} (\mu_{e''} - \mu_{e'}) \quad (1.55)$$

Since $\phi'' - \phi'$ equals the open-circuit voltage (E_{oc}) and

$$\mu_{e'} = \mu_{e'}^{Pt} = \mu_{e''}$$

we get

$$E_{oc} = \frac{1}{4F} \int_{\mu_{O_2}'}^{\mu_{O_2}''} t_{O_2} d\mu_{O_2} \quad (1.56)$$

The more general form of the above equation is

$$E_{oc} = \frac{1}{4F} \int_{\mu_{O^{2-}}'}^{\mu_{O^{2-}}''} d\mu_{O^{2-}} \quad (1.57)$$

This equation forms the basis for the thermodynamic measurements using solid electrolytes. In most such measurements $t_{ion} \geq 0.99$.

Stability of the electrolyte

While the potential utility of the solid electrolyte is greatly dependent upon the magnitude and selectivity of the ionic conductivity, its practical utilization in galvanic cells also requires that it meets the requirements of stability at the electrode potentials. This is a particularly important matter since many of the advanced galvanic cells utilize highly reducible cathodes and oxidizable anodes. It is not enough to know the voltage at which a phase decomposes, which establishes its electrolyte limit. In addition, the actual values of the limiting potentials in the galvanic cell environment need to be known in order to assess its stability in conjunction with the specific electrode materials, each of which establish characteristic reduction /oxidation potentials at the electrode / electrolyte interface. In the case of binary phases, the stability range can be computed from the Gibbs free energies of formation of adjacent phases. The situation is rather complicated for the ternary electrolyte. From an electrochemical stand point, the stability of the solid electrolyte in a given galvanic cell is estimated using cyclic voltammetry, wherein the solid electrolyte is polarized to extreme positive and negative potentials in a cell comprising inert but electrocatalytic metals such as noble metals, carbon as current collector.

6.2 Determination of Thermodynamic parameters by Conventional Methods

The important parameters necessary for a reasonable thermodynamic description of any system are a) specific heat as a function of temperature and pressure ii) enthalpy and entropy of formation and iii) phase diagrams in the case of solid solutions. The rest of the properties may be evaluated by using various thermodynamic relations. Some of the methods for evaluating the above parameters are outlined below.

Specific heat or heat capacity

The heat capacity of a body is defined as the amount of heat required to raise its temperature by one degree, i.e. specific capacity

$$C^* = \lim_{\Delta T \rightarrow 0} (\Delta Q / \Delta T) \quad (1.58)$$

The specific capacity is similarly defined as

$$c = c^* / m$$

where m is the mass of the body. The molar specific heat C is given by

$$C = CXM$$

where ' M ' is the molecular weight of the body. From the first law of thermodynamics, it is clear that the specific heat of a body at constant volume is the temperature derivative of its internal energy U , i.e.,

$$C_v = \left(dU / dT \right)_v \quad (1.59)$$

A knowledge of C_v would thus tell us the manner in which the internal energy is distributed among the different modes of thermal excitation. Such a knowledge as a function of temperature would provide information about supersonic solids, which have high degree of disorders and mostly undergo disorder-order type transformations.

The experimental determination of C_v presents problems for solids in terms of maintaining constancy of volume. On the other hand, maintaining a constant pressure would be easy. Hence, the specific heat at constant pressure is often measured and is related to C_v by

$$C_p - C_v = V_m \alpha^2 T / \beta \quad (1.60)$$

where V_m is the molar volume, ' α ' is the thermal volume expansion coefficient and β is the compressibility. In the absence of a precise value of β at all temperatures, Nernst-Lindemann empirical relation,

$$C_p - C_v = A C_p^2 T = V_m \alpha^2 T / \beta \quad (1.61)$$

can be used. Here A is a constant evaluated from V_m , α and β at any temperature. A large number of experimental methods have been described in the literature [119'120]. Such measurements fall broadly into two categories.

Drop methods: A heated sample is dropped into a calorimeter which measures the heat released ($-\Delta Q$). The heat released by the sample is measured as a sum of heat gained by the calorimeter and radiation losses. In a variation of this method, the equilibrium time is reduced by using a calorimeter whose temperature remains constant at the phase transformation of one of its components (e.g. Bunsen ice calorimeter).

Electrical heating method: A known amount of heat is supplied to the sample by an electrically heated resistance wire and the resulting change in temperature is measured. Either an isothermal or adiabatic calorimeter could be used. The latter

is more widely used and contains no temperature gradient across the reaction chamber and the jacket.

A comprehensive account of the various solid electrolytes, the conduction mechanism, an assessment of the errors involved in the emf measurements and their applications have been given by Schlömann^[115].

6.3 Comparison of Solid Electrolyte Method with Other Methods for Thermodynamic Measurements

Characterization of oxide systems can be done by a measurement of the enthalpies of formation by calorimetric method and a determination of free energies of formation either by the equilibration of the system with a gas mixture of known oxygen partial pressure or by emf method. The former method involves errors related to the phase changes during cooling (quenching) for a chemical/physical analysis of the equilibrated phases. The latter method, on the other hand, permits direct measurement of thermodynamic parameters at the temperature of the experiment with no quenching. Also, the emf method is quicker and more accurate within 1 mV (or 92 cal) as compared to 100-200 cal in the high temperature measurements. Obvious choice from the oxide thermodynamic measurements would be zirconia-based electrolyte for moderate oxygen partial pressures and thorium-based electrolytes for low oxygen partial pressures^[121]. Either an isothermal or adiabatic calorimeter could be used. The latter is more widely used and contains no temperature gradient across the reaction chamber and the jacket.

6.4 Kinetic Measurements

In kinetic studies, the current through the electrochemical cell is non-zero. The oxide ion current density is given by

$$I_{O^{2-}} = \frac{\sigma_{O^{2-}}}{2F} \frac{d\eta_{O^{2-}}}{dx}$$

Since

$$d\mu_{O^{2-}} - 2 d\mu_e = \frac{1}{2} d\mu_{O_2}$$

and

$$\eta_i = \mu_i + z_i F \phi$$

we get

$$I_{O^{2-}} = \frac{\sigma_{O^{2-}}}{2F} \left(\frac{d\mu_{O^{2-}}}{dx} + \frac{2d\mu_e}{dx} - 2F \frac{d\phi}{dx} \right) \quad (1.62)$$

The above current density of oxygen ions is related to the ionic current i_{ion} in the external measuring circuit through

$$I_{O^{2-}} = -\frac{i_{ion}}{A}$$

where 'A' is the cross sectional area of the electrolyte. Combining the above two equations and integrating from $x = 0$ to $x = L$, we obtain

$$E_{cell} = \frac{1}{4F} \int_{\mu_{O^{2-}}}^{\mu_{O_2}} d\mu_{O_2} + i_{ion} \Omega_{ion} \quad (1.63)$$

where

$$\Omega_{ion} = \frac{1}{A} \int_{x=0}^{x=L} \frac{1}{\sigma_{O^{2-}}} dx$$

is the ionic resistance of the electrolyte and $E_{cell} = \phi'' - \phi'$. This equation forms the basis for kinetic measurements using solid electrolyte cells.

6.5 Factors Limiting the Applicability of Solid Electrolyte Cells for Thermodynamic/Kinetic Measurements

- At ionic transport number $t_{ion} < 0.99$, the electronic conduction in the electrolyte is significant to cause problems in maintaining the desired chemical potentials at the electrode/electrolyte interface. In solid oxide electrolytes, however, there is useful range of oxygen pressure and temperature where $t_{ion} > 0.99$.
- Even at low short circuit currents, the emf though stable, contains an overvoltage due to a shift in the oxygen potential at the interface as a result of oxygen transfer.
- Reactions between the electrode and electrolyte are often complicated by the formation of a layer of reaction product.
- Studies at low oxygen pressures are to be preferably carried out in inert atmosphere (He or Ar), instead of vacuum, after ensuring that the flow rate of the inert gas has no effect on the measured emf.
- Slow equilibration of the electrode constituents limited by the sluggish diffusional processes.

- f) Polarization effects at the electrode/electrolyte interfaces are to be adequately accounted for.
- g) Electrode porosity/ homogeneity: A definite study on the effect of density on the partial conductivities of the sintered compacts hasn't been made. However, sintered compacts with 95 % theoretical density seem to be acceptable for most thermodynamic and kinetic applications. Low density electrolytes might permeate gases leading to unsteady emfs. Inhomogeneities in the electrolyte can lead to localized regions of enhanced electronic transference number (10-2). Finally, the solid electrolyte tends to exhibit a high degree of susceptibility to cracking under temperature gradients and thermal cycling.
- f) Experimental uncertainties: The accuracy of the measured Gibbs free energy is high due to a high accuracy possible in the measurements of cell emfs. The changes in the enthalpy and entropy measured from the variation of cell emf with temperature are relatively inaccurate due to the differential quotient dE/dT . Nevertheless, these values are superior to the calorimetric data. It is, however, possible that the measurements on the solid electrolyte cells are often complicated by instrument-related problems such as polarization of the cell due to low input impedance of the voltmeter/recorder and electrical pick up due to the improper shielding of the lead wires and/or grounding of the instruments.

7.0 REFERENCES

- 1) Heyne, L. in *Fast ion Transport in Solids*, cd. W. van Gool, North Holland, Amsterdam, 1973.
- 2) Wiedersich, H and Geller, S in *The Chemistry of Extended Defects in Non-metallic Solids*, cd. L. Eyring and M. O'Keefe, North Holland, Amsterdam, 1971.
- 3) Lidiard, A. B. in *Handbuch der Physik*, cd. S. Flugge Vol. 20, Springer-Verlag, Berlin, 1957, p. 246.
- 4) Phillips, J. C., J. Electrochem. Soc., 123,924 (1976).
- 5) Raleigh, D. O. (1976) in *Electrode Processes in Solid State Ionics*, cd. M. Kleitz and J. Dupuy, D. Reidel Pub. Co., Holland.
- 6) Weidersich, H. and Geller, S.,(1977) in *The Chemistry of Extended Defects in Non-Metallic Solids* (cd., L. Eyring and M.O' Keefe), North-Holland, Amsterdam.
- 7) Whittingham, M. S., and Silbernagel, B. G. in Solid Electrolytes (cd., P. Hagenmuller and W. van Gool) , Academic Press, New York 1978
- 8) Chandra, S. (1981), "*Supersonic Solids: Principles and Applications*", North-Holland, Amsterdam.
- 9) Wadsley, A. D., in *Non-Stoichiometric Compounds*, cd. L. Mandelcorn, Academic Press, New York, (1964), Ch. 3.
- 10) Kummer, J. T., in *Progress in Solid State Chemistry*, Vol. 7, eds. H. Reiss and J. O. McCaldin, Permaon Press, New York, 1972, p. 141.
- 11) Steele, B.C. H and Alcock, C. B., *Trans. Metall. Soc. AIME*, 233, 1359 (1965).
- 12) Wagner, C (1953), *J. Chem. Phys.*, 21, 1819.
- 13) Kiukkola, K. and Wagner,C(1957a) *J. Electrochem. Soc.*, 14,308.
- 14) Kiukkola, K. and Wagner, C (1957 b), *J. electrochem. Soc.*, 104,379
- 15) Bradley, J. N. and Greene P. D. (1966) *Trans. Faraday Soc.*, 62, 2069; Bradley, J. N. and Greene P. D. (1967a) *Trans. Faraday Soc.*, 63,424.
- 16) Bradley, J. N. and Greene, P. D., (1967b) *Trans. Faraday Soc.*, 63,2516.

- 17) Owens, B. B. and Argue, G. R., (1967), *Science*, 157,308.
- 18) Yao, Y. F. Y., and Kummer, J. T. (1967), *J. Inorg. Nucl. Chem.*, 29,2453.
- 19) Radzilowski, R. H., Yao, Y. F., and Kummer, J. T. (1969), *J. Appl. Phys.*, 40, 4716.
- 20) Weber, N. and Kummer, J. T. (1967), *Proc. Arm. Power Sources Conf.*, 21,37.
- 21) Coetzer, J. (1986), *J. Power Sources*, 18, 377;
- 22) Bones, R. J., Coetzer, J., Galloway, R. C. and Teagle, D. A. (1987), *J. Electrochem. Soc.*, 134,2379.
- 23) Bones, R., Teagle, Brooker, S. D. and Cullen, F. L. (1989), *J. Electrochem. Soc.*, 136, 1361.
- 24) Raleigh, D. O. (1967), *Solid State Electrochemistry, Progr. Solid State Chem.* 3, 83.
- 25) Heyne, L., (1 970) *Electrochim. Acts* 15, 1251;
- 26) Owens, B. B. (197 1) *Adv. Electrochem. Electrochem. Engg.*, 8, 1
- 27) Steele, B.C. H.(1972) in "Solid State Chemistry" (L. E. J. Roberts, cd.), p. 117, Butterworths, Washington D. C.
- 28) Whittingham, M. S. and Huggins, R. A. (1972), in "Solid State Chemistry" (R. S. Roth and S. J. Schneider, eds.), p. 139, Nat. Bur. Std. Spec. Pub]. 364, Washington
- 29) Hladik, J. (cd.) (1972), "Physics of Electrolytes" Vols. 1 and 2, Academic Press, New York;
- 30) van Gool, W. (1973) in "Fast Ion Conduction in Solids", (W. van Gool, cd), p. 201, North-Holland Publ. Amsterdam.
- 31) van Gool, W. (1974a), in "Phase Transitions, 1973" (H. K. Henisch, R. Roy and L. E. Cross,eds.), p. 373, Pergamon, Oxford.
- 32) van Gool, W. (1974b), *Ann. Rev. Mater. Sci.*, 4, 311.
- 33) Huggins, R. A. (1975) in "Diffusion in Solids: Recent Developments", (A. S. Nowick and J. J. Burton, eds.) p445, Academic Press, New York.
- 34) Huggins, R. A. (1977), *Adv. Electrochem. Electrochem. Engg.*, 10,323.

- 35) Steele, B.C. H. and Dudley, G. J. (1975), in "Solid State Chemistry", (L. E. J. Roberts, ed.) Ser. 2, p. 181. Butterworths, Washington D. C.
- 36) Holzapfel, G. and Rickert, H. (1975), in "Festkörperprobleme" (H. J. Queisser, ed.) Vol. 15, p. 317, Pergamon, Oxford.
- 37) Mahan, C. D. and Roth, W. L. (eds.) (1976) "Superionic Conductors", Plenum Press, New York.
- 38) Tubandt, C. and Lorenz, E. (1914) *Z Phys. Chem.*, 87, 513.
- 39) Funke, K. (1976), *Progr. Solid State Chem.*, 11, 345.
- 40) Hardy, J. P. and Flocken, J. W. (1970) *CRC Crit. Rev. Solid State Sci.*, 1, 605.
- 41) Johnson, J. W. (1964), *Phys. Rev.*, 136, a284.
- 42) Johnson, O. W., Pack, S. H., and DeFord, J. W. (1975a), *J. appl. Phys.*, 46, 1026.
- 43) Johnson, O. W., DeFord, J. W. and Pack, S. H. (1975b), in "Mass Transport in Ceramics" (A. R. Cooper and A. H. Heuer, eds.) p. 253, Plenum Press, New York.
- 44) Halstead, K., Benesh, W. U., Gullivar, R. D. H. and Huggins, R. A. (1973), *J. Chem. Phys.*, 58, 3530.
- 45) Dryden, J. S. and Wadley, A. D. (1958), *Trans. Faraday Soc.*, 54, 1574.
- 46) Singer, J., Kautz, H. E., Fielder, W. L., Fordyce, J. S. (1973) in "Fast Ion Transport in Solids; Solid State Batteries and Devices" (W. van Gool ed.), p. 153. North-Holland Pub., Amsterdam.
- 47) Beyeler, H. U., Hibma, T. and Schuler, C. (1977), *Electrochemical. Acts*
- 48) Johnson, R. T., Morosin, B., Knotek, M. L. and Biefeld, R. M. (1975c) *Bull. Am. Phys. Soc.*, 20, 330.
- 49) Johnson, R. T., Biefeld, R. M., Knotek, M. L. and Morosin, B. (1976), *J. Electrochem. Soc.*, 123, 680.
- 50) Raistrick, I. D., Ho, C. and Huggins, R. A. (1976), *J. electrochem. Soc.*, 123, 1469.
- 51) von Alpen, U., Rabenau, A., Talaat, G. (1977), *Appl. Phys. Lett.*, 30, 621.

- 52) Carter, R. E. and Roth, W. L. (1968) in "*Electromotive Force Measurements in High Temperature Systems*" (C. B. Alcock, ed.) p. 125. Institute of Mining and Metallurgy, London.
- 53) Etsell, T. H. and Flengas, S. N. (1970) *Chem. Rev.*, 70,339.
- 54) Kvist, A., (1972), in "*Physics of Electrolytes*", Vol. 1, ed. J. Hladik, Academic press, New York, Ch. 8.
- 55) Schoonman, J., Dirksen, G. J., and Blasse, G. (1973), *J. Solid State Chem.*, 7,245.
- 56) Derrington, C. E., and O'Keefe, M. (1973), *Nature, (London) Phys. Sci.*, 246, 44.
- 57) Kennedy, J. H., Miles (1976), *J. Electrochem. Soc.*, 123,47.
- 58) Benz, R. (1975), *Z. Phys. Chem.*, 95,25.
- 59) Liang, C. C. and Joshi, A. V. (1975) *J. Electrochem. Soc.*, 122,467.
- 60) Reau, J. M., et al., (1975), *C. R. Acad Sci. Paris (C)*, 280,225.
- 61) Kennedy, J. H., Miles, R. and Hunter, J (1973), *J. Electrochem. Soc.*, 120, 1441.
- 62) Halff, A. F. Schoonman and Rykclenkamp, A. J. H. (1973), *J. Phys. Chem.*, 34, C 9.
- 63) Hwang, T. Y., Engelsberg, M., Lowe, I. J. (1975), *Chem. Phys. Lett.*, 30,303.
- 64) Mahajan, M. and Rae, B. D. N. (1971), *Chem. Phys. Lett.*, 10,29.
- 65) Joshi, A. V. and Liang, C. C. (1975), *J. Phys. Chem. Solids*, 36,927.
- 66) Bonne, R. W. and Schoonman, J. (1977). *J. Electrochem. Soc.*, 124,28.
- 68) Huggins, R. A. (1977), *Electrochem. Acts.*, 22,733.
- 67) Raistrick, I. D., Ho., Ch., Hu, Y. W and Huggins, R. A. (1977), *J. Electroanal. Chem.*, 77,319.
- 69) Kennedy, J. H. (1977), in "*Solid Electrolytes*" (S. Geller, ed.) Springer Verlag, Berlin, p. 105.
- 70) Collogues, R. Thery, J., Boilot, J. P., (1978), in "*Solid Electrolytes*", (P. Hagenmuller and W. van Gool, eds.) Academic Press, New York, p. 253.

- 71) Tiller, C. O., Lilly, A. C. and LaRoy, B. C. (1 973), *Phys.. Rev.*B8, 4787.
- 72) Takahashi, T. Iwahara, Hand Ishikawa, T. (1 977), *J. Electrochem. Sot.*, 124,280.
- 73) Boukamp, B. A. and Huggins, R. A. (1976), *Phys. Lett*, 58A, 231.
- 74) Rabenau, A. and Shultz, H., (1976), *J. Less Common Metals*, 50, 155.
- 75) Geller, S.(1 967), *Science*, 157,310.
- 76) West, A. R. (1973), *J. Appl. Electrochem.*, 3,327.
- 77) Liebert, B. E. and Huggins, R. A. (1976) *Mater. Res. Bull*, 11,533.
- 78) Beniere, F (1972) in *Physics of Electrolytes*, ed. J. Hladik, Academic Press, New York.
- 79) Glyde, H. 1<.(1967), *Rev. Mod. Phys.*, **39,373**.
- 80) Rice, M. J. and Roth, W. L., (1972) *J. Soild State Chem.*, 4, 294(1972).
- 81) Druger, S. D., Ratner, M. A., and Nitzan, A, (1983) *Solid State Ionics* 9/10 11 15;
- 82) Druger, S. D., Ratner, M. A., and Nitzan, A, (1 983) *J. Chem. Physics.*, 79,3133.
- 83) Druger, S. D., Ratner, M. A., and Nitzan, A, (1985) *Phys. Rev.*, B, 313939.
- 84) Crank, J. (1956) "*The Mathematics of Diffusion*", Oxford University Press, London.
- 85) Carslaw, H.S. , Jaeger, J.C. (1959), "*Conduction of Heat in Solids*", Oxford University Press, London.
- 86) Einstein, (1905), *Annalen der Physik* (4), 17,549.
- 87) Hartley, G. S., (1 931), *Trans. Faraday Sot.*, 27, 10.
- 88) Wagner, C.(1957),*Proc. Intern. Comm. Electrochem. Thermodyn. Kinet.*, 7,361.
- 89) Wagner, C., (195 1), *Atom Movements*, Am. Society Metals, p. 153 Cleveland 1951.
- 90) Jest, W., (1952) in *Diffusion in Solids, Liquids and Gases*, Academic Press, New York.

- 91) Manning, J. R., (1968) "*Diffusion kinetics for Atoms in Crystals*", D. Van Nostrand Co Inc., New York.
- 92) Nowick, A. S., and Burton, J. J., (1975) (eds), *Diffusion in Solids*, Academic Press, New York.
- 93) Bannet, M. H., (1981), *Mat. Res. Sot. Symp. Proc.*, Vol 3, p.3 "*Nuclear and Electron Resonance Spectroscopy Applied to Materials Science*, " cd. by E. N. Kaufman and G. K. Shenoy, Elsevier.
- 94) Weppner, W., and Huggins, R. A., (1978), *Ann. Rev. Mater. Sci*, Vol 8, p269.
- 95) Rapp, R. A and Shores, D. A, (1970) in "*Techniques of Metals Research* ", Vol. 4, part 2, ed. R. A. Rapp, Interscience, New York, pp 123.
- 96) Blumenthal, R. N. and Scitz, M. A., (1974) in "*Electrical Conductivity in Ceramics and Glass*", cd. N. M. Tallan, Marcel Dekker, New York, Part a, 35.
- 97) Grahame, D. C., (1952) *J. Electrochem. Sot.*, 99,350 C.
- 98) Macdonald, J. R., (1976) in "*Electrode Processes in Solid State Ionics*" cd. M. Kleitz and J. Dupuy, Reidel Publishing Co., Dordrecht-Holland, p. 149.
- 99) Areher, W. I and Amstron R. D. , *Electrochemistry*, Specialist Periodical Reports Vol.7 , The Chemical Society, London (1976).
- 100) Bauerle , J. E,(1969) *J. Phys.Chem. Solids*, 30,2657.
- 101) Hodge, I. M., Ingram, M. D., and West, A. R., (1976), *J. Electroanal Chem.*, 74, 125.
- 102) Cole, K. S., and Cole, R. H. (1941), *J. Phys Chem.*, 9,341.
- 103) Wagner, C (1956), *Z. Elektorchem*, 60, 4-7.
- 104) Hebb, M. H. (1952), *J. Chem. Phys.*, 20, 185.
- 105) Spiro, M. (1970), in "*Techniques of Chemistry*", Vol. 1, part II (eds. A. Weissberger and B. W. Rossiter), Wiley, New York.
- 106) Leveque, M., Le Nest, J. F, Gandini, A. and Charadame, H. (1983), *Makromol. Chem. Rapid Commun.*, 4,497.

- 107) Leveque, M., Le Nest, J. F, Gandini, A. and Charadame, H. (1985), *J. Power Sources*, 14,27.
- 108) Sorensen, P. R. and Jacobsen, T. (1982), *Electrochim. Acts*, 27, 1671.
- 109) Tubandt, C. (1932) in "*Handbuch der Experimentalphysik*" Vol. Xii. Part I (Eds. W. Wein, and F. Harms), Akademie Verlag, Leipzig.
- 110) Bouridah, A., Dalrd, F., Deroo , D. and Armand, M. B. (1986), *Solid State Ionics*, 18/19, 287.
- 111) Bloosky, P. M., Shriver, D. F., Austin, P. and Allcock, H. R. (1986), *Solid State Ionics*, 18/19, 258.
- 112) Watanabe, M., Sanui, K., Ogata, N., Kobayashi, T. and Ohtaki, Z. (1985), *Z. Appl. Phys.*, 57, 123.
- 113) Fauteux, D. (1985), *Solid State Ionics*, 17, 133.
- 114) Bruce, P. G. and. Vincent, C. A (1987), *J. Electroanalytical Chem.*, 225, 1
- 115) Schmalzried, H. (1972) in "*Metallurgical Chemistry*", *Proc. Symp. of Natl. Phys. Labs.*, Middlesex, U. K., p. 39.
- 116) Peters, H. and Mobius, H. (1958) *Z. Phys. Chem.* 209,298.
- 117) Peters, H. and Mann, G. (1959) *Z. Electrochem.*, 63,244
- 118) Wagner, C. (1933), *Z. Phys. Chem.*, B 21,25 (1933).
- 119) Keesom, P. H. and Pearl man, N. (1959) in *Methods of Experimental Physics*, Vol VI, *Solid State Physics*, (cd. K. Lark Horovitz and V. A . Johnson) Academic Press, New York.
- 120) Sherwood, E. M., (1967) in *High Temperature Materials and Technology*, cd. I. E. Campbell and E. M. Sherwood, John Wiley, New York.
- 121) Steele, B. C. H., in *Emf Measurements at High Temperature*, (Ed. C. B. Alcock, institution of Mining and Metallurgy, London (1968)p.16.

LIST OF SYMBOLS

n_+ , n_-	: number of positive and negative ion vacancies
N	: number of cation or anion sites
x	: mole fraction; distance co-ordinate
C	: mole fraction of impurity; concentration, mol cm^{-3}
ω	: angular frequency of sinusoidal wave form; jump frequency of ions/vacancies
ν_0	: vibrational frequency, Hz
σ	: conductivity, $\text{Ohm}^{-1}\text{cm}^{-1}$
μ	: partial molal free energy; electrochemical potential
J	: flux of species, $\text{moles cm}^{-2}\text{s}^{-1}$
j, I	: current density, A cm^{-2}
D	: diffusion coefficient, cm^2s^{-1}
γ	: activity coefficient
B	: absolute mobility, $\text{cm}^2\text{J}^{-1}\text{s}^{-1}$
λ	: jump length, cm
E	: single electrode potential, Volt
t_i	: transference number
ϕ	: electric potential ; phase angle
z	: impedance
z'	: real component of complex impedance
Z''	: imaginary component of complex impedance

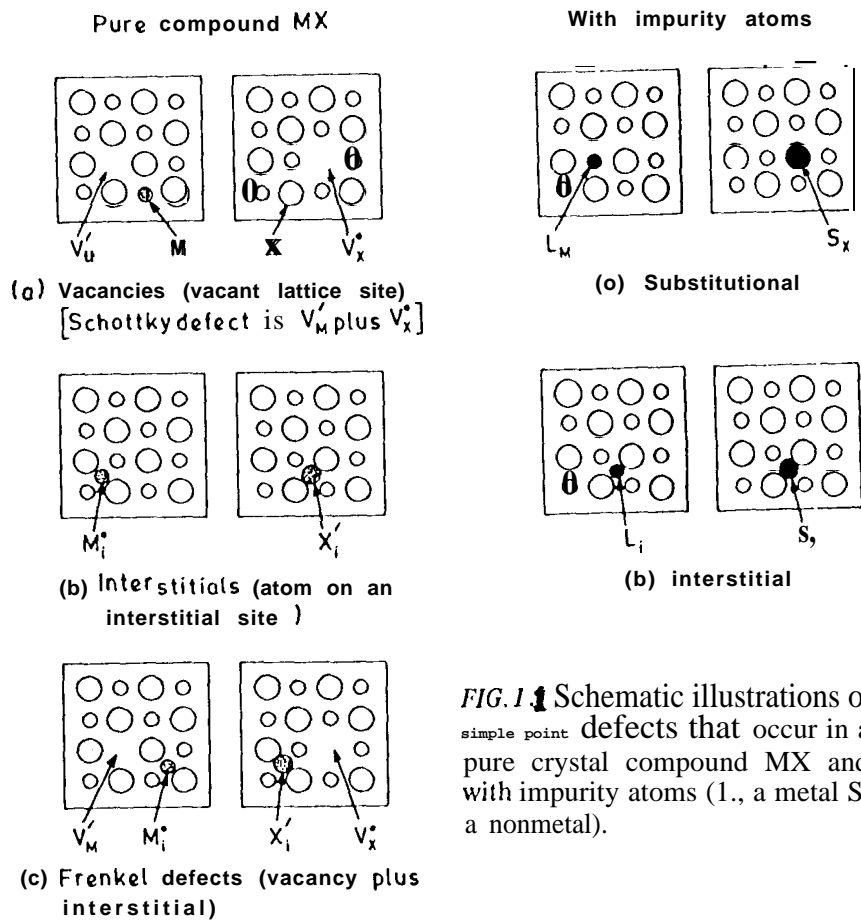


FIG. 1 Schematic illustrations of simple point defects that occur in a pure crystal compound MX and with impurity atoms (I., a metal S, a nonmetal).

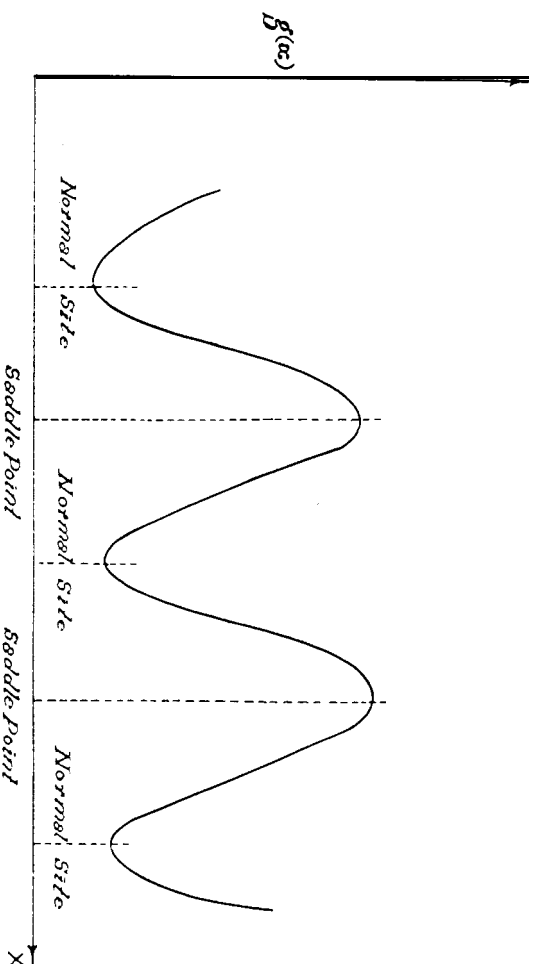


Fig 1.2 Energy along jump direction with no applied gradient.

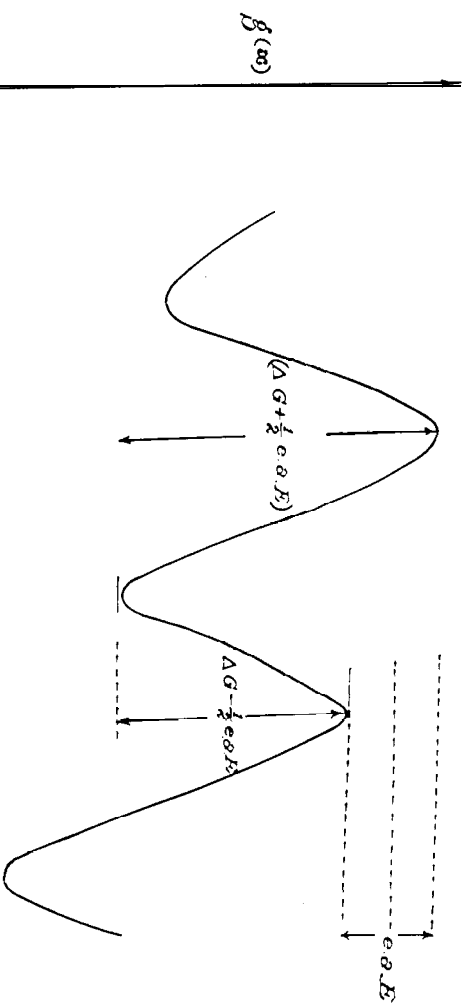


Fig 1.3 Energy along jump direction when electric field gradient is applied.

Table 1 Summary of defects in ionic crystals

Type of substance and examples	Structure	Defect structure and transport mechanisms
Alkali halides LiF, NaCl, KI, etc.	NaCl (f.c.c.)	Schottky defects. Cation vacancies more mobile.
Cesium halides, CsI, TlCl, etc.	CsCl (s.c.)	Schottky defects. Anion vacancies more mobile.
Silver halides AgCl, AgBr, etc.	NaCl (f.c.c.)	Cation Frenkel defects. Cation motion by both vacancy and interstitialcy.
Alkaline earth halides CaF_2 , SrCl_2 , etc.	fluorite and others	Anion Frenkel defects. Anion vacancy and interstitial both mobile.
Other halides PbBr_2 , LaCl_3 , etc.	various	Schottky defects.
Simple salts with complex anions NaN_3 , Ag_2SO_4	low symmetry	Cation Frenkel defects.
Alkaline earth oxides	wurtzite and NaCl	Schottky defects. Cation concentration controlled by impurities.
Fluorite structure UO_2 , ZrO_2 : CaO	fluorite	Anion Frenkel defects.
Transition metal oxides FeO , Cr_2O_3	various	Cation diffusion by vacancies. Oxygen diffusion by dislocations.
Divalent chalcogenides ZnS , PbTe	NaCl and others	Neutral Frenkel defects, both cation and anion.
Small cations and large anions AgI , RbAg_4I_5 , Li_2SO_4 , etc.	mostly cubic	Cation disorder.

Fig. 1.4 : Equivalent circuits for the electrode/ electrolyte interface

